ACS Sustainable Chemistry & Engineering

Research Article

pubs.acs.org/journal/ascecg

Effect of Carbon Dots on Conducting Polymers for Energy Storage Applications

Balamurugan Devadas[†] and Toyoko Imae[*,†,‡]

[†]Graduate Institute of Applied Science and Technology, National Taiwan University of Science and Technology, 43 Section 4, Keelung Road, Taipei 10607, Taiwan

[‡]Department of Chemical Engineering, National Taiwan University of Science and Technology, 43 Section 4, Keelung Road, Taipei 10607, Taiwan

ABSTRACT: The influence of carbon dots (Cdots) in conducting polymers (polypyrrole (PPy) and polyaniline (PANI)) was investigated toward high specific capacitance. Herein, a viable in situ chemical oxidative polymerization method was employed to synthesize the polymer@Cdots composites. The enhancements of specific capacitance and long-term stabilities of PPy@Cdots and PANI@Cdots are due to the synergistic effect of polymers and Cdots. Thus, the Cdots in the composite enhanced more than double the capacitance of original polymers: The specific capacitances of composites were 676 and 529 F/g for PPy@Cdots and PANI@Cdots, respectively, at current density of 1 A/g. This report indicates the remarkable capacitance intension and the desirable durability reinforcement of pseudocapacitors by the easy addition of less-conductive carbon material.

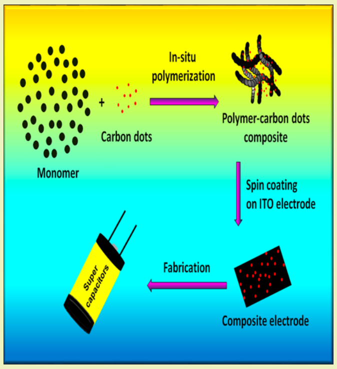

KEYWORDS: *Carbon dot, Polypyrrole, Polyaniline, Pseudocapacitance, Specific capacitance, Durability*

INTRODUCTION

The world population growth and the continuous use of many devices including vehicles and various electronic machineries and appliances are stimulating the improvement of alternative energy devices in facing the environmental crisis. Among the numerous energy devices, electrochemical energy storage devices, especially supercapacitors, are considered promising next generation power devices owing to their desirable properties of extraordinary power density, energy storage capacity, fast charging ability, ecofriendliness, and long-term stability.[1,2] Supercapacitors have been used in many systems such as portable electronic devices, electric vehicles, power backup for mobile devices, air bags, etc.[3,4]

On the basis of the electrode materials and their performances, supercapacitors are mainly categorized as electrical double layer capacitors (EDLCs) and pseudocapacitors.[5] Though pseudocapacitors have higher energy density and specific capacitance than EDLCs, pseudocapacitor-based energy devices have suffered from practical applications owing to their deficiencies such as poor cycling and mechanical stability.[6,7] In this respect, there is a real necessity to advance drawbacks of the pseudocapacitors. Henceforth, a hybrid of pseudocapacitors with EDLC is the first priority to improve the power density, long-term cycle stability, and wide operating potential window of supercapacitors.[8] Hitherto, the carbon materials (EDLC, nonfaradaic process), metal oxides/hydroxides, and conducting polymers (pseudocapacitors, faradaic process) are known as electrode materials for supercapacitors.[9−11]

Carbon quantum dots (Cdots) are the fluorescent nanosized carbon particles pioneered by Xu et al.[12] in 2004. Fundamentally, the Cdots possess the sp^2 graphitic core structure with oxidized functionalities. Hence, the Cdots with semiconducting properties are capable of replacing the semiconductor quantum dots and can help the fast charge tunnelling on optoelectronic devices.[13] Different from other carbon materials (graphene, carbon nanotube, etc.), carbon dots (Cdots) are an extremely economical, hydrophilic, and small (2−5 nm) carbon family material, which can consist of desired functional groups including hydroxyl, carboxyl, amine, and carbonyl groups, depending on the raw materials.[14,15] These functional moieties on the surface of Cdots impart the excellent water solubility and chemical reaction and can be modified with other polymeric, organic, and inorganic materials. This modification enhances the physicochemcial properties of both Cdots and modification materials.[16]

Basically, Cdots have great potential for use in the biological units (bioimaging, biosensor, medicine/drug delivery, etc.), since its strong fluorescent and photophysical properties.[17,18] In addition, owing to the physicochemical assets of Cdots, they have received great attention in diverse applications including chemical sensing, photocatalysis, and electrocatalysis.[16] More excitingly, the keen interaction of Cdots in the nanocomposites enhances the electron transport and ionic motion in the

Received: June 9, 2017
Revised: October 7, 2017
Published: November 4, 2017

DOI: 10.1021/acssuschemeng.7b01858
ACS Sustainable Chem. Eng. 2018, 6, 127−134

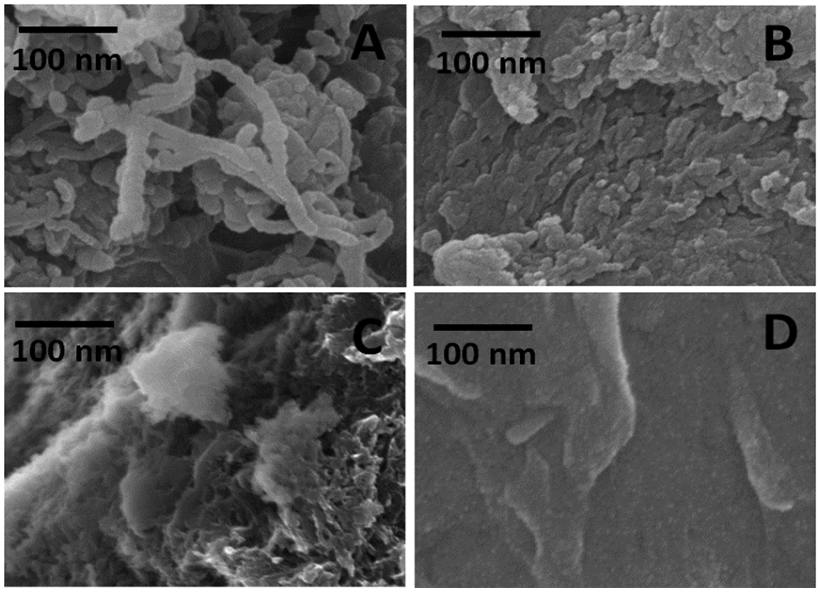

Figure 1. FESEM images of (A) PPy, (B) PPy@Cdots(1:1), (C) PANI, and (D) PANI@Cdots(1:0.4).

supercapacitor charge/discharge process, and it is stimulating fast redox reactions and high specific capacitance.[19] More recently, the Cdot-based hybrid materials have been reported for their applications for supercapacitors.[20−22] To date, a variety of materials, such as biomass derived carbon, 2D graphene, and metal−organic frameworks, are attracting great attention in the field of energy storage applications.[23,24] Those electrode materials exhibit excellent specific capacitance and good cycle life. However, the synthesis procedure of these materials involves a multistep process, need of toxic chemicals, and high cost. Hence, readily obtainable materials are demanded for energy storage application.

On the other hand, conducting polymers (CPs) such as polypyrrole (PPy) and polyaniline (PANI) are hitherto known to be the most efficient pseudocapacitance materials for supercapacitors.[2] These polymers are mainly preferred for energy storage applications due to the following reasons: high specific capacitance, high charge conductivity, high surface area, active reversible reaction, high intrinsic flexibility, low cost, and easy route to make films.[25,26] Despite many benefits of CPs, their low mechanical stability and cycle life result in poor charge/discharge capability.[27,28] In this context, coupling of CPs with carbon materials possessing the highly conducting and the high surface area as a nanocomposite can result in enhanced stable specific capacitance.[29,30] The synergistic relationship between CPs and carbon materials aids in enhancing the supercapacitor abilities of such materials.[31] Hitherto, there have been several reports using CPs/graphene and/or single walled carbon nanotube hybrid materials for supercapacitor applications.[32−36] Nonetheless, the hybrids of CPs and Cdots are judicious choices and will be new materials with high cycle stability and promising electrochemical performance. Indeed, there is no report of the use of this combination for supercapacitors.

By combining pseudocapacitor materials with nanosized quasi-zero-dimensional carbon materials, the functionality of the materials can be significantly enhanced. In this respect, nanocomposites of CPs (PPy and PANI) and less-conductive Cdots as electrode materials for supercapacitors were developed in this study. There are some challenges to overcome with regard to synthesis procedure to derive the synergistic effect of hybrid materials, and electrode fabrication was advanced in this investigation. The composites of PPy@Cdots and PANI@Cdots were synthesized via in situ chemical polymerization using cetyltrimethylammonium bromide (CTAB) surfactant and ammonium persulfate (APS) oxidizing agent. The influence of Cdots on the CPs for the specific capacitance enhancement was evaluated.

■ EXPERIMENTAL SECTION

Materials. Pyrrole and aniline (99% extra pure), CTAB, APS (98%), citric acid, and ethylenediamine were purchased from Acros organics, Belgium. Hydrochloric acid (37%) was purchased from Scharlab, Spain. Sodium chloride pellets were procured from Yakuri Pure Chemicals Co. Ltd., Japan. Ethyl alcohol (99.5%) was obtained from Choneye Pure Chemicals, China. All of the chemicals were of analytical grade and used as received. All of the experimental solutions were prepared by doubly distilled deionized water. Indium tin oxide (ITO)-coated glass substrates were purchased from Aimcore Technology, Taiwan.

Synthesis of Polymer@Cdots Composites. A hydrothermal method[15] was used to synthesize Cdots.[37] Citric acid (1 g) was dissolved in water (10 mL), and ethylenediamine (300 μL) was added to this solution. Then, the calculated molar ratio of $COOH/NH_2$ was 1/1. The solution mixture was heated in an autoclave at 230 °C for 4 h, and then the temperature of the reaction vessel was cooled to room temperature. The dark brown Cdots solution was then used to prepare polymer@Cdots composites.

The composites of Cdots with conducting polymers (PPy and PANI) were synthesized using CTAB and APS.[38] CTAB (124 mg, 0.01 M) was dissolved in aqueous 0.1 M hydrochloric acid solution (30 mL) under stirring, and as-synthesized Cdots solution (0.2, 0.5, or 1 mL) was mixed in this solution. Sequentially, pyrrole monomer (0.06 mL, 0.025 M) was added to the Cdot-containing CTAB solution under stirring at 0−5 °C, and the stirring was continued for another 30 min. Finally, APS in aqueous HCl solution (6 mL, 0.025 M) was added dropwise into this mixture under a temperature maintained at 0−5 °C, and the mixed solutions were constantly stirred for 1 day. Then, the black PPy@Cdots composite was collected by filtration through a cellulose acetate membrane filter (0.2 μm), washed several times with water and ethanol, and dried at 50 °C for 12 h. The calculated weight ratio of monomer/raw material of Cdots was 1:0.4, 1:1, and 1:2. The same procedure was followed for the preparation of

PANI@Cdots composites by using aniline as a monomer. Thus, hereafter, composites are mentioned: polymer@Cdots(1:x, x = 0.4, 1, and 2). As controls, PPy and PANI were prepared using the same procedure but without adding Cdots.

Measurements. Field-emission scanning electron microscope (FESEM) studies were performed using JP JEOL model JSM-6500F (Japan). Fourier transform infrared (FT-IR) absorption spectroscopic measurements were performed using a Nicolet 6700 instrument (Japan). Ultraviolet−visible (UV−vis) absorption spectroscopic analyses were carried out using a Jasco Corporation Model V-670 EX (Japan). Thermogravimetric analysis (TGA) was performed with a TGA Q 500 series, TA appliance (USA), at an increasing heating level of 10 °C/min. The electrochemical measurements were carried out on an electrochemical workstation (ZAHNER messsysteme, model XPot, Germany) using a conventional three electrode system. A polymer@Cdots-coated ITO plate working electrode, an Ag|AgCl reference electrode, and a platinum wire counter electrode were employed, and the measurements were performed at the scan rates of 100 to 5 mV/s over the potential range from −0.4 to 0.8 V in 1 M NaCl electrolyte solution.

For the preparation of working electrodes, the ITO-coated glass substrate (2 cm × 1 cm) was cleaned well using detergent, acetone, and finally water and, in addition, by photochemical exposure for 10 min in vacuum UV light to decompose organic contaminants. After polymer@Cdots composites were dispersed in ethanol by ultrasonication (Bransonic Ultrasonics Model B1210J-DTH, Japan) for 2 h, the composites were uniformly coated on clean ITO glass by spin coating at 500 rpm for 10 s and additionally by 1500 rpm for 30 s. The polymer@Cdots-coated ITO glass was dried at 50 °C for 1 h and then used as a working electrode for electrochemical studies. The polymer-coated ITO electrodes were also prepared with the same amount as polymer@Cdots (0.06 mg/cm^2).

■ RESULTS AND DISCUSSION

Characterization of Polymer@Cdots. The surfactant-assisted in situ polymerization was carried out in the presence of Cdots, and PPy@Cdots and PANI@Cdots composites were synthesized. The SEM images of pristine polymers and as-synthesized composites are shown in Figure 1. The PPy possessed a long flexible chain structure. The surface morphology of PANI was nonstructured, and both polymers had a rough surface. However, when polymers were synthesized in the presence of Cdots, the surface of polymer@Cdots composites became smoother and flatter than those of pristine polymers. However, it is difficult to distinguish the Cdots in the polymers@Cdots composites from the SEM images shown in Figure 1B,D because of the small size (around 5 nm) of Cdots and similar X-ray density to that of the polymer matrix. Additionally, small Cdots can be embedded within the void volume of the polymer matrix to flatten the surface of composites.

The FT-IR spectroscopic investigation was confirmed for identifying chemical structures of Cdots, polymers, and polymer@Cdots(1:1) composites, and characteristic IR bands are shown in Figure 2 and listed in Table 1. IR absorption bands of Cdots at 3440, 1650, 1555, and 1391 cm^{-1} can be attributed to the characteristic bands of raw materials (citric acid and ethylenediamine) and of the produced graphitized group.[22] On the other hand, the characteristic IR bands of PPy were confirmed at 1550, 1454, 1293, 1170, 1037, and 789 cm^{-1}. An IR spectrum of the PPy@Cdots composite was like that of PPy except for one weak absorption band at 3440 cm^{-1} corresponding to an O—H stretching vibration mode of Cdots. However, there were differences in shifts of some PPy bands: The shifted C═C and C—N stretching vibration bands of pyrrole in PPy@Cdots indicate the interaction between PPy and Cdots. A similar result was obtained even on the PANI composite: Both PANI and PANI@Cdots displayed IR bands of quinoid and benzenoid rings, but a characteristic band of Cdots at 1650 cm^{-1} was not recognized and the C═C stretching band (1550 cm^{-1}) of PANI quinoid ring was shifted in the composite, indicating the interaction of PANI with Cdots. It may be interpreted that the deprotonation of carboxylic acid in free Cdots occurred on the process of

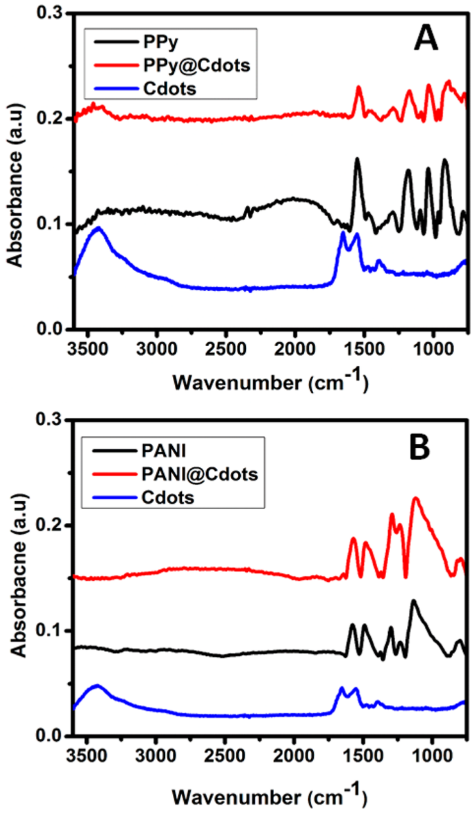

Figure 2. FT-IR absorption spectra of Cdots, polymers, and polymer@Cdots(1:1) composites: (A) PPy and (B) PANI series.

Table 1. FT-IR Absorption Bands of Cdots, Polymers, and Polymer@Cdots(1:1) Composites

assignment[a]	Cdots	PPy	PPy@Cdots
νOH	3440		3445
νC═O	1650		
νNH, νC═C (pyrrole)	1555	1550	1540
νC—N (pyrrole and benzenoid ring)		1454	1465
νC═C	1391		
δC—N		1293	1289
νC—H (pyrrole ring)		1170	1168
δC—H		1037	1031
γC—H		789	775
assignment[a]	Cdots	PANI	PANI@Cdots
νOH	3440		
νC═O	1650		
νNH, νC═C (quinoid ring)	1555	1550	1568
νC═C (benzenoid ring)		1480	1477
νC═C	1391		
νC—N		1293	1293
(N═Q═N) (Q: quinoid ring)		1094	1110

[a] Vibration mode: ν; stretching, δ; in-plane deformation, γ; out-of-plane deformation.

electrostatic hybridization with polymer in composites, although IR bands of deprotonated carboxylate overlapped with bands of polymers.

Figure 3 displays the thermal stability analysis of Cdots, polymers, and polymer@Cdots(1:1) under N_2 atmosphere. Initial (below 100 °C) weight loss in all materials was due to the evaporation of adsorbed small molecules like water. Successive weight loss from 250 to 730 °C was from the continuous decomposition of PPy (see Figure 3A). These thermal behaviors are common for general organic molecules. On the other hand, part of the Cdots were decomposed at the first drop, and the second weight loss of Cdots happened above 900 °C, although there were residual (28 wt %) Cdots even at 1000 °C. Organic groups like carboxylic acid and amine could be burned-out at the first drop, but the thermal behavior above 900 °C indicates the existence of graphitized components in Cdots, being similar to carbon nanotubes and other carbon materials.[39] The thermal profile of composites of polymers with Cdots behaves like Cdots, and then, this result confirms the coexistence of Cdots with polymer in composites.

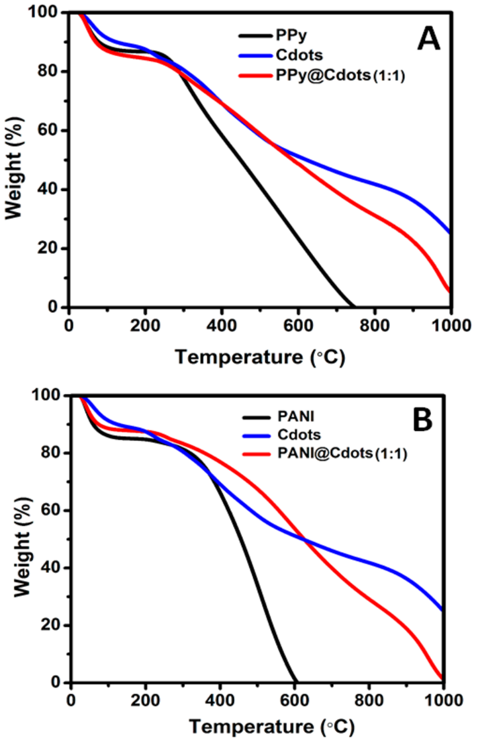

Figure 3. TGA analysis of (A) Cdots, PPy, and PPy@Cdots(l:1), and (B) Cdots, PANI, and PANI@Cdots(1:1) under N_2 atmosphere.

As in PPy, the first step decomposition of PPy@Cdots(1:1) occurred at 250−550 °C. While at 750 °C there was complete weight loss of PPy, the weight loss of PPy@Cdots(1:1) was only 65 wt %. However, different from the weight loss of PANI from 250 to 630 °C, the first step decomposition of PANI@Cdots(1:1) happened at a higher temperature (see Figure 3B). This phenomenon indicates the strong interaction of PANI and Cdots.

Supercapacitor Performance. The CV curves for polymer- and polymer@Cdots-modified working electrodes were recorded at the various scan rates of 5 to 100 mV/s over the potential range from −0.4 to 0.8 V in 1 M NaCl electrolyte solution, as displayed in Figure 4A−D. Both polymers and polymer@Cdots composites exhibit redox-couple type CV curves in this potential range, indicating pseudocapacitance behavior. Moreover, the integral area of the CV curve of the PPy@Cdots composite was larger than that of pristine PPy. In contrast, the PANI@Cdots electrode exhibited a slightly larger integral area than that of a PANI electrode but smaller than that of a PPy@Cdots electrode.

These results revealed that Cdots enhance the electrical conductivity and specific capacitance of both PPy and PANI. Moreover, it is worth noting that the pseudocapacitor behavior still existed in the polymer@Cdots composites. This result indicates that Cdots in the composites significantly enhanced the pseudocapacitance performance of polymers, although Cdots exhibited extremely low current density and did not show a redox peak (data not shown). Thus, polymer@Cdots composites are related to pseudocapacitor behavior rather than hybrid capacitors (EDLC + pseudocapacitors).

The specific capacitance Cs can be calculated using eq 1

$$\mathrm{Cs} = \int I \, \mathrm{d}V / \nu m \Delta V \tag{1}$$

The term $\int I \, \mathrm{d}V$ is the integral area of the CV cycle, and ν is the scan rate. m is the mass of materials loaded on the ITO glass substrate, and ΔV is the potential range. The specific capacitance values of all the modified electrodes were calculated at different scan rates (from 100 to 5 mV/s) and displayed in Figure 4E,F. The specific capacitance of all electrodes commonly increased with decreasing scan rate, but the capacitance values depended on electrodes. The initial addition of Cdots to polymers increased the specific capacitance of polymers, but the excess addition of Cdots deduced the specific capacitance of polymers. The amount of Cdots inducing the maximum performance was a 1:1 weight ratio for PPy and lower (1:0.4) for PANI than PPy. Then, the specific capacitance of composite electrode at 5 mV/s was 754 F/g for PPy@Cdots(1:1) against 300 F/g of the PPy electrode and 568 F/g for PANI@Cdots(1:0.4) against 256 F/g of PANI: They were higher than double the values for pristine polymers.

The optimum enhancing effect of Cdots on the pseudocapacitor occurred at limited Cdot contents. On the in situ polymerization, Cdots may interact with monomers, and they are effectively incorporated in polymers during the polymerization. The Cdots embedded in the polymer network act as a junction between polymer networks and improve electron transfer between conducting polymer networks through graphitized structures of Cdots, leading to the promotion of high capacitance performance. However, this process will break down at the excess additional amount of Cdots, because a high amount of less-conductive Cdots may inhibit the conductivity of polymers, reducing the intrinsic electroactivity of polymers. This result in the present investigation is related to the previous report, where a high content of Cdots reduced the specific surface area of the original material.[16] Thus, the effective performance occurs at the limited amount of Cdots.

In the case of PPy, the composite at 1:1 displayed the best performance, but a high enough performance was achieved at the Cdots content of 1:0.4 in PANI. Here, the long alkyl chain cationic CTAB and anionic APS can be self-assembled and act as templates for the formation of a PPy nanostructure.[40] The key advantage is that Cdots are well-dispersed in the reaction solution containing a self-assembly of CTAB and APS. Why are there differences in the amount of Cdots enhancing the electroactivity of polymers? The reason should be the affinity of

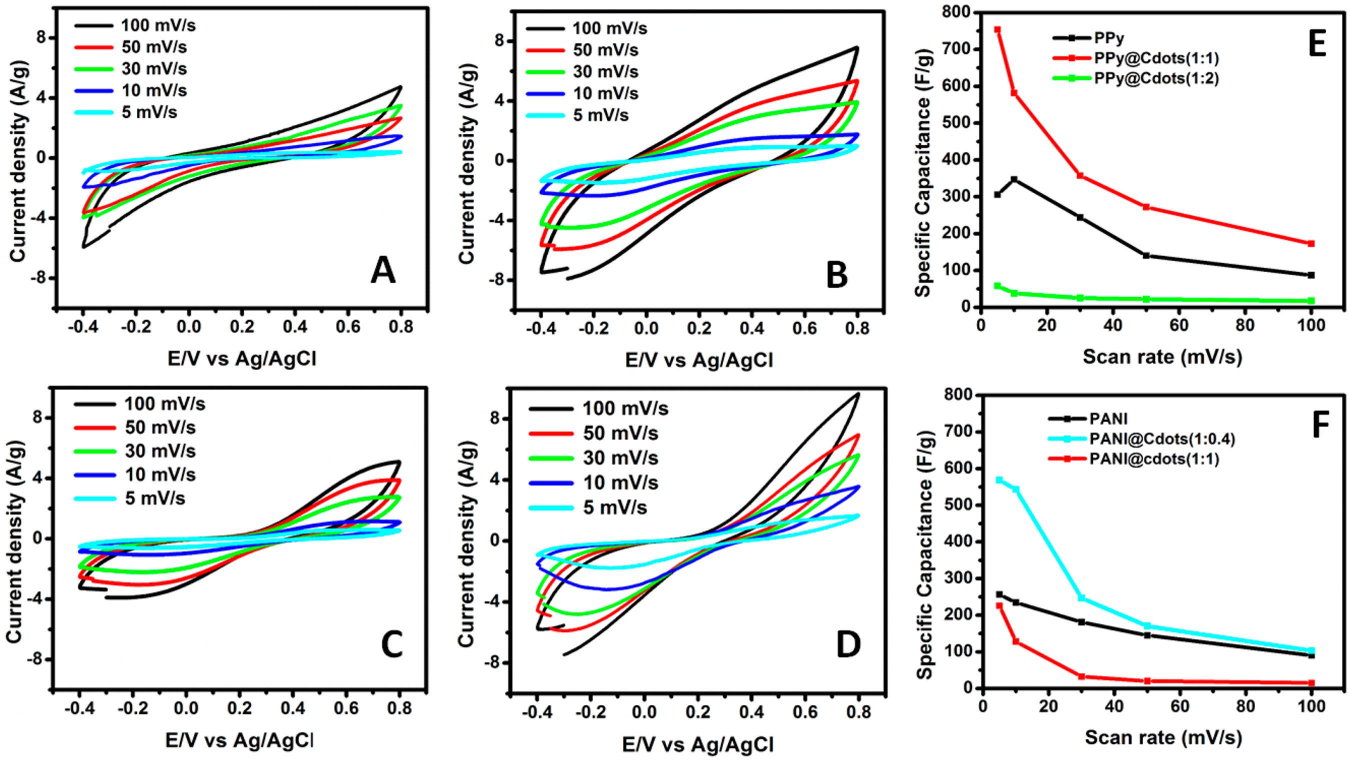

Figure 4. CV curves of (A) PPy, (B) PPy@Cdots(1:1), (C) PANI, and (D) PANI@Cdots(1:0.4) at different scan rates. Specific capacitance of (E) PPy, PPy@Cdots(1:1), and PPy@Cdots(1:2), and (F) PANI, PANI@Cdots(1:0.4), and PANI@Cdots(1:1).

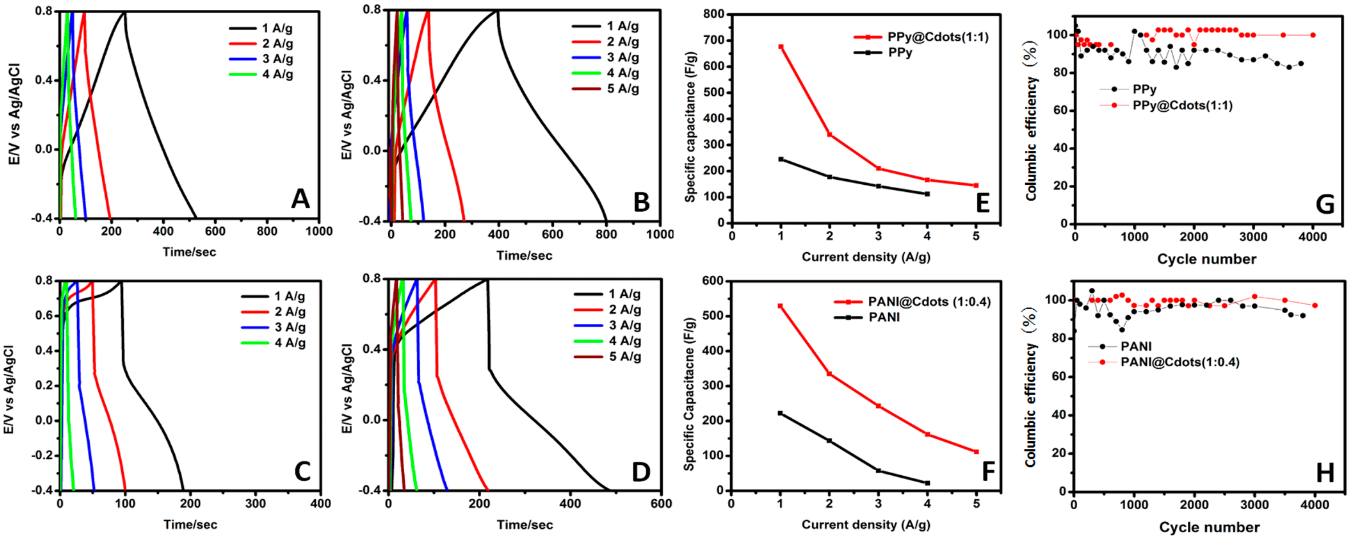

Figure 5. GCD curves of (A) PPy, (B) PPy@Cdots(1:1), (C) PANI, and (D) PANI@Cdots(1:0.4) at different current densities specific capacitance of (E) PPy and PPy@Cdots(1:1), and (F) PANI and PANI@Cdots(1:0.4). Coulombic efficiency of (G) PPy and PPy@Cdots(1:1) and (H) PANI and PANI@Cdots(1:0.4).

Cdots to self-assemble CTAB and APS and to generate polymers. The functional and graphitized groups of Cdots can play major roles in the interaction with them. In the case of PPy@Cdots, the possible interaction is a hydrogen bond attraction between the carboxylic acid group of Cdots and the amine group of PPy.[40] On the other hand, the conjugated bonding and quinoid N-active sites of PANI can facilitate the affinity of PANI with Cdots:[41] The PANI@Cdots composites are designed not only by hydrogen bonding but also by possible attraction between the aromatic ring of PANI and graphitized structure of Cdots. Thus, Cdots can strongly adsorb in the vicinity of PANI than PPy and results in the high performance of PANI at the addition of smaller amount of Cdots than PPy.

To confirm the charge capacity of the as-prepared composites, the galvanostatic charge and discharge (GCD) characteristics of PPy, PPy@Cdots(1:1), PANI, and PANI@Cdots(1:0.4) were investigated at different current densities with potential range of −0.4 to 0.8 V and shown in Figure 5A–D.

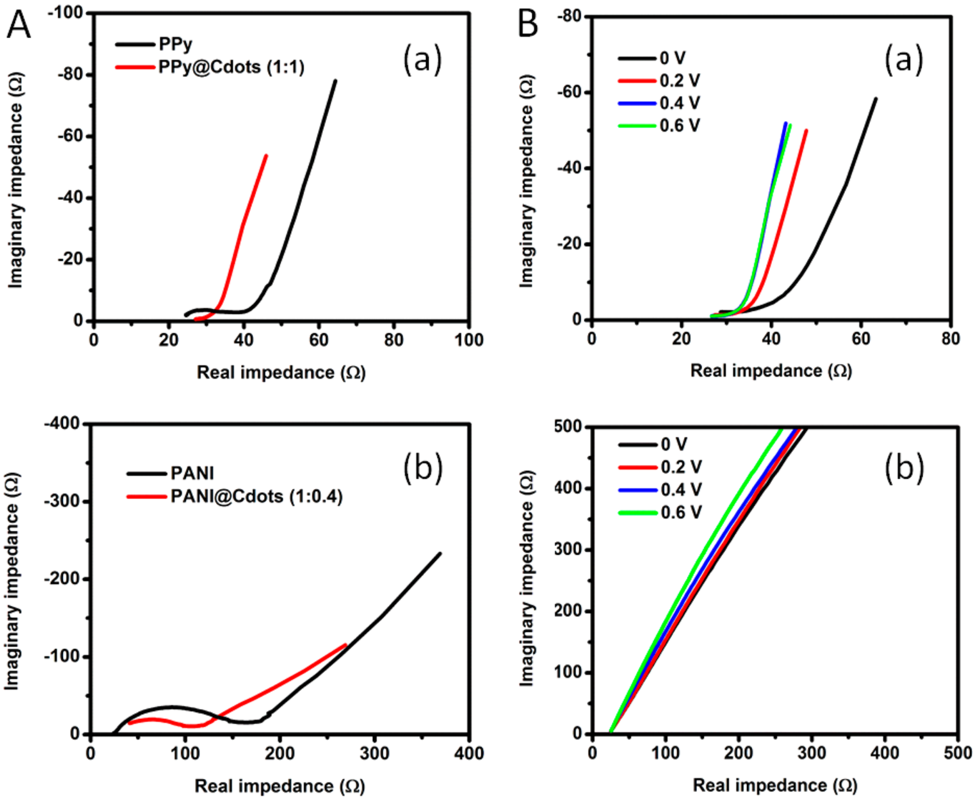

Figure 6. (A) EIS spectra of (a) PPy and PPy@Cdots(1:1) and (b) PANI and PANI@Cdots(1:0.4). (B) EIS spectra of (a) PPy@Cdots(1:1) and (b) PANI@Cdots(1:0.4) at 0, 0.2, 0.4, and 0.6 V.

The specific capacitance Cs from GCD method can be calculated using eq 2

$$\mathrm{Cs} = (I\mathrm{dt})/(m\mathrm{dV}) \tag{2}$$

The term I is the applied current, and dt is the discharging time. m is the mass of material, and dV is the potential window. The calculated capacitance at 1 A/g was 245 and 222 F/g for pristine polymers (PPy and PANI), respectively, and 676 and 529 F/g for PPy@Cdots(1:1) and PANI@Cdots(1:0.4), respectively (see Figure 5E,F). These values were smaller (82%, 87%, 90%, and 93%, respectively) than the capacitance at 5 mV/s from CV curves for the corresponding electrodes. These results reveal that the specific capacitance values of both polymer composites were larger than those of pristine polymers because of the synergistic effect of the addition of Cdots, consistent with the results from CV analysis described above.

Moreover, the Coulombic efficiency (η) can be calculated using charging and discharging currents from GCD curve based on eq 3:[42]

$$\eta = \Delta t_{\mathrm{d}}/\Delta t_{\mathrm{c}} \tag{3}$$

where the terms Δt_{d} and Δt_{c} are the discharging and charging times, respectively. Then, the Coulombic efficiency is one of the parameters in supercapacitors to study the cycle stability of materials and devices. The Coulombic efficiencies of PPy@Cdots(1:1) and PANI@Cdots(1:0.4) were measured up to 4000 cycles and compared with that of polymers (Figure 5G,H). Pristine polymers showed the Coulombic efficiency of 85.2% and 91.8% for PPy and PANI, respectively, indicating less stability for conductive polymer electrodes. This behavior is common for polymer pseudocapacitors. However, the PPy@Cdots(1:1) composite electrode exhibited 99.2% efficiency after 4000 cycles. Similarly, the PANI@Cdots(1:0.4)-modified electrode showed 97.5% efficiency after 4000 cycles. Thus, it can be indicated that the capacitance was stable even after 4000 cycles for both polymer@Cdots composites, and conducting polymers strengthened the stability by hybridizing with Cdots.

The conductivity and charge transfer rate studies were performed using electrochemical impedance spectroscopy (EIS) on glassy carbon electrode (GCE). Figure 6A shows EIS curves of polymers and polymer@Cdots in 1 M NaCl with an applied frequency range from 100 mHz to 100 kHz at open circuit potential. The semicircle region indicates the electron transfer resistance (R_{ct}) of the corresponding material. The impedance R_{ct} value was fitted using the Randles circuit model. Relating to polymers, the polymer@Cdots composites showed less of a semicircle, revealing the low electron transfer resistance. The R_{ct} values of composite electrodes were 30 Ω for PPy@Cdots(1:1) against 36 Ω of PPy and 94 Ω for PANI@Cdots(1:0.4) against 148 Ω of PANI. These results suggest that polymer@Cdots have a faster electron transfer rate than that of pristine polymers. Thus, the Cdots significantly enhance the conductivity of polymers, agreeing with CV results. Moreover, the EIS spectra of polymer@Cdots composites were collected for different potentials (0, 0.2, 0.4, and 0.6 V) (Figure 6B). Almost similar R_{ct} values (~30 Ω for PPy@Cdots(1:1) and ~29 Ω for PANI@Cdots(1:0.4)) were found for different potentials. The same resistance values at different potentials indicate the excellent electrochemical capacitance in the applied potential range for polymer@Cdots composites.[42] This result is in good agreement with the previous report for polyaniline and graphene composites.[43]

Table 2 compares the specific capacitance values of Cdots-hybridized composite electrodes obtained by other research

Table 2. Comparison of Capacitance Performance of Present Material to Other Reported Material

electrode material	specific capacitance (F/g) without Cdots at 5 mV/s and 1A/g	specific capacitance (F/g) with Cdots at 5 mV/s and 1A/g	amount of Cdots	ref
PPy@Cdots	300 and 245	754.1 and 676	1:1 wt ratio	this work
PANI@Cdots	256 and 222	568.6 and 529	1:0.4 wt ratio	this work
MnO_2/Cdots/graphene		280	0.3 mg	20
activated carbon/Cdots	100	134	6 wt %	21
Cdots/reduced graphene oxide	121	211.9	5:1 mass ratio	22
carbon quantum dots/PPy/TiO_2	241	440 at 20 mV/s		44
PPy/sulfonated graphene composite		360		45
carbon bundle fiber/PPy-reduced graphene oxide		130.81		46
PANI/carbon nanotube		324		47
PANI/few layered graphene-coated activated carbon fiber		400.17		48

groups. When the other Cdots-hybridized composite electrodes were compared with the present electrodes, the present electrodes exhibited higher specific capacitance values and higher performance effects than those of other reported hybrid electrodes. The specific capacitance of the carbon quantum dots/PPy/TiO_2 electrode measured at 20 mV/s was still lower than the estimated 470 F/g of the present PPy@Cdots at 20 mV/s. The specific capacitor of PANI/few layered graphene-coated activated carbon fiber electrode was quite high but still lower than that of PANI@Cdots.

CONCLUSIONS

In summary, Cdots enhanced the specific capacitance and stability of polymer pseudocapacitors. The reported in situ chemical oxidative polymerization method was the effective procedure to exert the synergistic effect between polymers and Cdots. Thus, the specific capacitance values of both polymers increased up to double or more by addition of an adequate amount of Cdots. Moreover, as the most important result, the contribution of Cdots eliminated the lessened durability of the polymer pseudocapacitor, which was the serious disadvantage. Thus, the polymer@Cdots hybrid is the ultimate choice as an electrode material for application to supercapacitors, and using polymer@Cdots as electrode materials is an excellent way to further the development of a prototype energy storage/conversion system.

AUTHOR INFORMATION

Corresponding Author

*E-mail: imae@mail.ntust.edu.tw.

ORCID

Toyoko Imae: 0000-0003-2731-1960

Author Contributions

The manuscript was written through contributions of all authors. All authors have given approval to the final version of the manuscript.

Notes

The authors declare no competing financial interest.

ACKNOWLEDGMENTS

B.D. appreciates the financial support from National Taiwan University of Science and Technology, Taiwan, for postdoctoral scholarship.

REFERENCES

(1) Lu, M.; Beguin, F.; Frackowiak, E. *Supercapacitors: Materials, Systems and Applications*; John Wiley & Sons, 2013.

(2) Shown, I.; Ganguly, A.; Chen, L. C.; Chen, K. H. Conducting polymer-based flexible supercapacitor. *Energy Sci. Eng.* **2015**, *3* (1), 2−26.

(3) Shi, F.; Li, L.; Wang, X. L.; Gu, C. D.; Tu, J. P. Metal oxide/hydroxide-based materials for supercapacitors. *RSC Adv.* **2014**, *4* (79), 41910−41921.

(4) Wei, H.; Zhu, J.; Wu, S.; Wei, S.; Guo, Z. Electrochromic polyaniline/graphite oxide nanocomposites with endured electrochemical energy storage. *Polymer* **2013**, *54* (7), 1820−1831.

(5) Guan, C.; Liu, J.; Wang, Y.; Mao, L.; Fan, Z.; Shen, Z.; Zhang, H.; Wang, J. Iron oxide-decorated carbon for supercapacitor anodes with ultrahigh energy density and outstanding cycling stability. *ACS Nano* **2015**, *9* (5), 5198−5207.

(6) Chen, S. M.; Ramachandran, R.; Mani, V.; Saraswathi, R. Recent advancements in electrode materials for the high performance electrochemical supercapacitors: a review. *Int. J. Electrochem. Sci.* **2014**, *9* (8), 4072−4085.

(7) Chen, T.; Dai, L. Carbon nanomaterials for high-performance supercapacitors. *Mater. Today* **2013**, *16* (7), 272−280.

(8) Zhang, F.; Zhang, T.; Yang, X.; Zhang, L.; Leng, K.; Huang, Y.; Chen, Y. A high-performance supercapacitor-battery hybrid energy storage device based on graphene-enhanced electrode materials with ultrahigh energy density. *Energy Environ. Sci.* **2013**, *6* (5), 1623−1632.

(9) Xiao, X.; Han, B.; Chen, G.; Wang, L.; Wang, Y. Preparation and electrochemical performances of carbon sphere@ZnO core-shell nanocomposites for supercapacitor applications. *Sci. Rep.* **2017**, *7*, 40167.

(10) De Oliveira, A. H. P.; Nascimento, M. L. F.; De Oliveira, H. P. Carbon Nanotube@MnO_2@Polypyrrole Composites: Chemical Synthesis, Characterization and Application in Supercapacitors. *Mater. Res.* **2016**, *19* (5), 1080−1087.

(11) Kim, B. K.; Sy, S.; Yu, A.; Zhang, J. Electrochemical supercapacitors for energy storage and conversion. *Handbook of Clean Energy Systems* **2015**, 1.

(12) Xu, X.; Ray, R.; Gu, Y.; Ploehn, H. J.; Gearheart, L.; Raker, K.; Scrivens, W. A. Electrophoretic Analysis and Purification of Fluorescent Single-Walled Carbon Nanotube Fragments. *J. Am. Chem. Soc.* **2004**, *126*, 12736−12737.

(13) De, B.; Karak, N. Recent progress in carbon dot−metal based nanohybrids for photochemical and electrochemical applications. *J. Mater. Chem. A* **2017**, *5*, 1826−1859.

(14) Liu, W.; Li, C.; Ren, Y.; Sun, X.; Pan, W.; Li, Y.; Wang, J.; Wang, W. Carbon dots: surface engineering and applications. *J. Mater. Chem. B* **2016**, *4* (35), 5772−5788.

(15) Prasannan, A.; Imae, T. One-pot synthesis of fluorescent carbon dots from orange waste peels. *Ind. Eng. Chem. Res.* **2013**, *52* (44), 15673−15678.

(16) Lim, S. Y.; Shen, W.; Gao, Z. Carbon quantum dots and their applications. *Chem. Soc. Rev.* **2015**, *44*, 362−381.

(17) Wang, J.; Qiu, J. A review of carbon dots in biological applications. *J. Mater. Sci.* **2016**, *51* (10), 4728−4738.

(18) Xu, Q.; Kuang, T.; Liu, Y.; Cai, L.; Peng, X.; Sreeprasad, T. S.; Zhao, P.; Yu, Z.; Li, N. Heteroatom-doped carbon dots: synthesis, characterization, properties, photoluminescence mechanism and biological applications. *J. Mater. Chem. B* **2016**, *4* (45), 7204−7219.

(19) Zhu, Y.; Ji, X.; Pan, C.; Sun, Q.; Song, W.; Fang, L.; Chen, Q.; Banks, C. E. A carbon quantum dot decorated RuO_2 network: outstanding supercapacitances under ultrafast charge and discharge. *Energy Environ. Sci.* **2013**, *6* (12), 3665−3675.

(20) Unnikrishnan, B.; Wu, C. W.; Chen, I. W. P.; Chang, H. T.; Lin, C. H.; Huang, C. C. Carbon Dot-Mediated Synthesis of Manganese Oxide Decorated Graphene Nanosheets for Supercapacitor Application. *ACS Sustainable Chem. Eng.* **2016**, *4* (6), 3008−3016.
(21) Kumar, V. B.; Borenstein, A.; Markovsky, B.; Aurbach, D.; Gedanken, A.; Talianker, M.; Porat, Z. Activated Carbon Modified with Carbon Nanodots as Novel Electrode Material for Supercapacitors. *J. Phys. Chem. C* **2016**, *120* (25), 13406−13413.
(22) Dang, Y. Q.; Ren, S. Z.; Liu, G.; Cai, J.; Zhang, Y.; Qiu, J. Electrochemical and Capacitive Properties of Carbon Dots/Reduced Graphene Oxide Supercapacitors. *Nanomaterials* **2016**, *6* (11), 212.
(23) Khan, A. H.; Ghosh, S.; Pradhan, B.; Dalui, A.; Shrestha, L. K.; Acharya, S.; Ariga, K. Two-Dimensional (2D) Nanomaterials towards Electrochemical Nanoarchitectonics in Energy-Related Applications. *Bull. Chem. Soc. Jpn.* **2017**, *90*, 627−648.
(24) Cao, X.; Tan, C.; Sindoro, M.; Zhang, H. Hybrid micro-/nano-structures derived from metal−organic frameworks: preparation and applications in energy storage and conversion. *Chem. Soc. Rev.* **2017**, *46*, 2660−2677.
(25) Snook, G. A.; Kao, P.; Best, A. S. Conducting-polymer-based supercapacitor devices and electrodes. *J. Power Sources* **2011**, *196* (1), 1−12.
(26) Ramya, R.; Sivasubramanian, R.; Sangaranarayanan, M. V. Conducting polymers-based electrochemical supercapacitors—Progress and prospects. *Electrochim. Acta* **2013**, *101*, 109−129.
(27) Shi, Y.; Peng, L.; Ding, Y.; Zhao, Y.; Yu, G. Nanostructured conductive polymers for advanced energy storage. *Chem. Soc. Rev.* **2015**, *44* (19), 6684−6696.
(28) Peng, C.; Zhang, S.; Jewell, D.; Chen, G. Z. Carbon nanotube and conducting polymer composites for supercapacitors. *Prog. Nat. Sci.* **2008**, *18* (7), 777−788.
(29) Fan, X.; Yang, Z.; He, N. Hierarchical nanostructured polypyrrole/graphene composites as supercapacitor electrode. *RSC Adv.* **2015**, *5* (20), 15096−15102.
(30) Chang, H. H.; Chang, C. K.; Tsai, Y. C.; Liao, C. S. Electrochemically synthesized graphene/polypyrrole composites and their use in supercapacitor. *Carbon* **2012**, *50* (6), 2331−2336.
(31) Liu, Y.; Wang, H.; Zhou, J.; Bian, L.; Zhu, E.; Hai, J.; Tang, J.; Tang, W. Graphene/polypyrrole intercalating nanocomposites as supercapacitors electrode. *Electrochim. Acta* **2013**, *112*, 44−52.
(32) Li, X.; Zhitomirsky, I. Electrodeposition of polypyrrole−carbon nanotube composites for electrochemical supercapacitors. *J. Power Sources* **2013**, *221*, 49−56.
(33) Lee, H.; Kim, H.; Cho, M. S.; Choi, J.; Lee, Y. Fabrication of polypyrrole (PPy)/carbon nanotube (CNT) composite electrode on ceramic fabric for supercapacitor applications. *Electrochim. Acta* **2011**, *56* (22), 7460−7466.
(34) Moussa, M.; El-Kady, M. F.; Zhao, Z.; Majewski, P.; Ma, J. Recent progress and performance evaluation for polyaniline/graphene nanocomposites as supercapacitor electrodes. *Nanotechnology* **2016**, *27* (44), 442001.
(35) Zhang, K.; Zhang, L. L.; Zhao, X. S.; Wu, J. Graphene/Polyaniline Nanofiber Composites as Supercapacitor Electrodes. *Chem. Mater.* **2010**, *22* (4), 1392−1401.
(36) Ahmed, M. M.; Imae, T. Electrochemical properties of a thermally expanded magnetic graphene composite with a conductive polymer. *Phys. Chem. Chem. Phys.* **2016**, *18* (15), 10400−10410.
(37) Krysmann, M. J.; Kelarakis, A.; Dallas, P.; Giannelis, E. P. Formation mechanism of carbogenic nanoparticles with dual photoluminescence emission. *J. Am. Chem. Soc.* **2012**, *134* (2), 747−750.
(38) Zhang, X.; Zhang, J.; Song, W.; Liu, Z. Controllable synthesis of conducting polypyrrole nanostructures. *J. Phys. Chem. B* **2006**, *110* (3), 1158−1165.
(39) Yadav, S. K.; Mahapatra, S. S.; Yadav, M. K.; Dutta, P. K. Mechanically robust biocomposite films of chitosan grafted carbon nanotubes via the [2+ 1] cycloaddition of nitrenes. *RSC Adv.* **2013**, *3* (45), 23631−23637.
(40) Zhang, B.; Xu, Y.; Zheng, Y.; Dai, L.; Zhang, M.; Yang, J.; Chen, Y.; Chen, X.; Zhou, J. A facile synthesis of polypyrrole/carbon nanotube composites with ultrathin, uniform and thickness-tunable polypyrrole shells. *Nanoscale Res. Lett.* **2011**, *6* (1), 431.
(41) Wang, H.; Lin, J.; Shen, Z. X. Polyaniline (PANi) based electrode materials for energy storage and conversion. *Journal of Science: Advanced Materials and Devices.* **2016**, *1* (3), 225−255.
(42) Yuan, C.-Z.; Gao, B.; Zhang, X.-G. Electrochemical capacitance of $NiO/Ru_{0.35}V_{0.65}O_2$ asymmetric electrochemical capacitor. *J. Power Sources* **2007**, *173* (173), 606−612.
(43) Fan, X.; Gao, H.; Zhong, L.; Xu, H.; Liu, J.; Yan, C. Investigation of the capacitive performance of polyaniline/modified graphite composite electrodes. *RSC Adv.* **2015**, *5*, 3743−3747.
(44) Xie, Y.; Du, H. Electrochemical capacitance of a carbon quantum dots−polypyrrole/titania nanotube hybrid. *RSC Adv.* **2015**, *5* (109), 89689−89697.
(45) Bora, C.; Sharma, J.; Dolui, S. Polypyrrole/sulfonated graphene composite as electrode material for supercapacitor. *J. Phys. Chem. C* **2014**, *118* (51), 29688−29694.
(46) Bashid, H. A. A.; Lim, H. N.; Kamaruzaman, S.; Rashid, S. A.; Yunus, R.; Huang, N. M.; Yin, C. Y.; Rahman, M. M.; Altarawneh, M.; Jiang, Z. T.; Alagarsamy, P. Electrodeposition of polypyrrole and reduced graphene oxide onto carbon bundle fibre as electrode for supercapacitor. *Nanoscale Res. Lett.* **2017**, *12* (1), 246.
(47) Simotwo, S. K.; DelRe, C.; Kalra, V. Supercapacitor Electrodes Based on High-Purity Electrospun Polyaniline and Polyaniline−Carbon Nanotube Nanofibers. *ACS Appl. Mater. Interfaces* **2016**, *8* (33), 21261−21269.
(48) Chu, H. J.; Lee, C. Y.; Tai, N. H. Three-dimensional porous polyaniline/graphene-coated activated carbon fiber electrodes for supercapacitors. *RSC Adv.* **2016**, *6* (112), 111465−111471.

DOI: 10.1021/acssuschemeng.7b01858